Thermal parameter estimation of mold in petri dishes by application of flashlight and thermal camera measurements

Luiz F. S. FERREIRA[1], Thomas PIERRE[2*], Leonardo A. B. VARON[3], Helcio R. B. ORLANDE[1]

[1] Université Fédérale de Rio de Janeiro, Politécnica/COPPE, Cidade Universitária, 68502, Rio de Janeiro, Brésil.
[2] Univ. Bretagne Sud, UMR CNRS 6027, IRDL, F-56100 Lorient, France.
[3] Univ. Santiago de Cali, Street 5 #62-00, Cali, Colombia.
[*](auteur correspondant : thomas.pierre@univ-ubs.fr)

Abstract – Microbiology standard procedures for bacteria or micro-organisms detection in liquid or gas media usually require incubation of the samples for a few days. This work is aimed at the fast detection of micro-organisms by photothermal excitation on a plate with culture media that containing molds. The temperature is measured with an infrared camera. Temperature variations during the cooling period are used for the solution of a parameter estimation problem. The lumped model parameter is estimated by Markov Chain Monte Carlo method via Metropolis-Hastings algorithm.

Nomenclature

Latin letters

A	area, m²
c_p	specific heat, J·kg^{-1}·K^{-1}
E	energy, J
h	heat transfer coefficient, W·K^{-1}·m^{-2}
$\boldsymbol{P}$	vector parameters
r	radius, mm
T	temperature, °C
t	time, s
$\mathbf{Y}$	measurement vector

Greek letters

α	Metropolis-Hastings ratio
ρ	density, kg·m^{-3}
ε	emissivity
σ	Stefan–Boltzmann constant, W·m^{-2}·K^{-4}
θ	nondimensional temperature
π	probability distribution function

1. Introduction

The process of bacteria and microorganisms detecting can take many hours or even days. There are an extensive set of techniques used to determine the viability of bacteria, such as nucleic acid-based methods, fluorescent dye-based methods, cellular/metabolic properties, and culture-based methods [1]. The European standard BS EN 14683 establishes minimum requirements for surgical masks used in operating rooms and other areas of healthcare facilities to avoid cross-contamination as much as possible. Therefore, a set of procedures is required to verify the adequacy of such masks in relation to several aspects. Among them, the procedure for calculating the bacterial filtration efficiency (BFE) is of interest, which is obtained by exposing plates to a device that sprays a solution with bacteria. After an incubation period of 48 hours at 37 ± 2 °C, the number of bacterial cultures for each plate is counted. These bacteria form on an agar gel Petri dish following a procedure of exposure to a Staphylococcus aureus culture diluted in peptone water. After the procedure described and counting the amount of bacterial culture in each plate, the average of the BFE of all plates is calculated, thus obtaining the filtration efficiency [2]. The complete work focuses on culture-based methods (CBM) to perform a count of the number of bacterial cultures that reproduce after the standardized test for respective regulation. But, for preliminary approach, the experimental apparatus and the algorithms are developed in order to detect, count, and estimate parameters for molds. The

https://doi.org/10.25855/SFT2023-024

objective of this work is to automatically detect microorganisms in a petri plate, more specifically mold/fungi given their larger magnitude when compared with bacterial cultures. After the detection, estimate thermophysical parameters and dimensions of these organisms.

2. Mathematical model and inverse problem

In this work, we use the inverse problem under Bayesian framework to estimate the thermal parameters for mold of different sizes in agar gel. This approach needs a direct problem and an inverse problem methodology, which is described in this section. The direct problem assumes heat exchange between the mold and the medium as a lumped heat transfer, which works quite well in small bodies with Biot number less than 0.1. In this modeling approach, the inner temperature depends on a simple energy balance between the body and the environment. Equation (1) shows this general energy balance:

$$dE\ /dt = E_{\mathrm{g}} - E_{\mathrm{conv}} - E_{\mathrm{rad}} \tag{1}$$

where the left-hand term is the stored energy in the volume, the first right-hand term is the heat generation considered negligible, the second is the energy lost by convection, and the third item is the energy lost by radiation. The heat losses are assumed only due to convective and radiative exchanges and negligible in the base of the hemisphere. An illustration of a hemisphere for modelling the mold geometry can be seen in Figure 1.

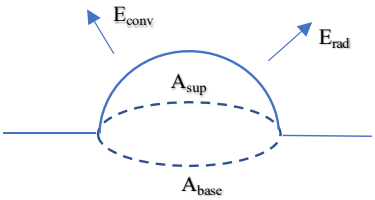

Figure 1: *Geometry of a hemisphere.*

Hence, we can write the direct problem as:

$$\rho c_p V\ dT\ /dt = -(h_r + h_L)A_s(T - T_\infty) \tag{2}$$

$$T(t = 0) = T_{ini} \tag{3}$$

where ρ is the density, c_p the specific heat, T_∞ is the room temperature (about 22 °C), T_{ini} the initial temperature, h_L convective heat transfer coefficient, and h_r is the linearized heat transfer coefficient for radiation, given by:

$$h_r \equiv 4\varepsilon\sigma {T_\infty}^3 \tag{4}$$

Despite h_r depends on the temperature, in the temperature range considered in our experiment, the variation for this coefficient is negligible but is considered in the uncertainties of the respective parameter. Considering the values of $V = 2\pi r^3/3$ and $A_s = 2\pi r^2$ for a hemisphere, and changing the variables using $h = h_r + h_L$, and $\theta(t) = T(t) - T_\infty$, the solution for equations (2) and (3) is the following expression:

$$\theta(t) = \theta_0 e^{-mt} \tag{5}$$

$$m = 3h\ /(\rho c_p r) \tag{6}$$

where $\theta_0 = T_{ini} - T_\infty$, ρc_p is the volumetric heat capacity, and r is the radius of the base for each mold.

The Bayesian approach for inverse problems deals with all available information to obtain the better estimative for parameters and its uncertainties taking into account prior information and the model selected to treat the measurements. All these elements are combined using the

Bayes' theorem (7). The statistical inversion approach is based in some principles: for example, all parameters in the model are considered random variables and the solution of the inverse problem is the posterior probability distribution [3]. Based on all information available for parameters **P** before the measured data is available, we need to select a probability distribution function $\pi(\mathbf{P})$ that represents the prior information. It is needed to select the likelihood function $\pi(\mathbf{Y}|\mathbf{P})$ for modelling the measurement errors and to develop methods to explore the posterior density function, which is the conditional probability distribution given the measurements $\pi(\mathbf{P}|\mathbf{Y})$.

$$\pi(\mathbf{P}|\mathbf{Y}) \propto \pi(\mathbf{Y}|\mathbf{P})\pi(\mathbf{P}) \tag{7}$$

The Metropolis-Hastings algorithm with separate sampling for the parameters is given by the following steps [3], [4]:

1. Let $t = 0$ and start the Markov chains with the sample $\mathbf{P}^{(0)}$.
2. Sample candidates $\boldsymbol{P}^*$ from the proposal distribution $q(\mathbf{P}^*|\mathbf{P}^{(t)})$.
3. Compute the Metropolis-Hastings ratio
$$\alpha(\mathbf{P}^*|\mathbf{P}^{(t)}) = \min\left[1, \pi_{post}(\mathbf{P}^*)q\left(\mathbf{P}^{(t)}|\mathbf{P}^*\right)/\left(\pi_{post}\left(\mathbf{P}^{(t)}\right)q\left(\mathbf{P}^*|\mathbf{P}^{(t)}\right)\right)\right]$$
4. Generate a random number with a uniform distribution in (0,1), $U \sim U(0,1)$.
5. If $U \leq \alpha(\mathbf{P}^*|\mathbf{P}^{(t)})$, make $\mathbf{P}^{(t+1)} = \mathbf{P}^*$. Otherwise, make $\mathbf{P}^{(t+1)} = \mathbf{P}^{(t)}$.
6. Make $t = t + 1$ and return to step 2 to generate the sequence $\{\mathbf{P}^{(1)}, \mathbf{P}^{(2)}, \ldots \mathbf{P}^{(n)}\}$.

The parameters of the mathematical model considered here are given by equation (8). As they are combined to form the parameter m in equation (6), they are correlated. The estimation of the sole parameter *m* should be enough, but it is been extended to the three parameters (8). The Bayesian inference gives the possibility to evaluate priors on parameters, what cannot propose deterministic techniques. The initial temperature θ_0 is considered a deterministic parameter. The priors are determined and presented in Section 3.

$$\mathbf{P} = \left[\rho c_p, h, r\right]^T \tag{8}$$

3. Materials and Methods

A thermographic camera FLIR SC660 records the images of a disposable petri plate with 90 mm diameter and 15 mm high containing about 15 ml of agar gel contaminated with several microorganisms initially uncharacterized. Contamination of the sterilized plate is performed by opening its lid to ambient air and storing it at an ambient temperature of 23 ± 2 °C for two days.

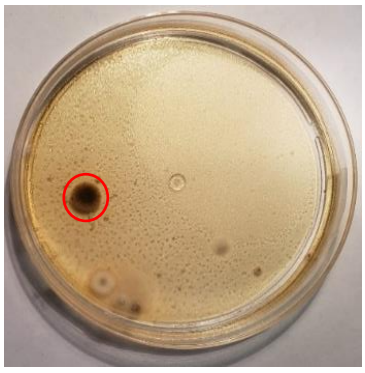

Figure 2: *Agar gel plate contaminated with mold and yeasts.*

Figure 3: *Experimental apparatus.*

Figure 2 shows the top view of the plate, with the variety of organisms that grows during the incubation period at the specified temperature. The experimental apparatus can be seen in

Figure 3, where the camera optical axis is perpendicular to the petri plate, and the flashlight is outside of camera field of vision. The plate is positioned between three plastic tips so that the image capture position remains the same. There are two height controls, and the camera focus can be done automatically or manually. The flashlight is provided by an emitter ATEK LLC 800 generally used in photography studios, positioned at the top next to thermal imaging camera.

Each pixel from the thermal image corresponds to one temperature measurement and these temperatures have associated uncertainties. The minimum element which forms the digital image, namely pixel, can represent different sizes for real objects depending on the distance between the lens and the object under analysis. The thermal camera used has 640 × 480 pixels with 7.5 – 13.0 μm of spectral range and accuracy of ± 1 °C or ± 2 % of reading. A microscope micrometer calibration ruler is used to estimate the pixels dimensions based on the captured thermal images. This ruler is showed in Figure 4. After several measurements, using all graduated scales for vertical and horizontal directions, a value for the basis (horizontally) of each pixel is obtained with mean value of 0.264 ± 0.040 mm. In the perpendicular position (vertically), the mean value is 0.27 ± 0.02 mm. The error propagation can be calculated to obtain the value for the area as 0.07 ± 0.01 $mm^2 \cdot pixel^{-1}$. These values are related strictly with the specific experimental apparatus, considering 40 cm between the lens and the plate image recorded. These calculations must be done every time that the experimental apparatus is changed, the distance between lens and plate and the focus configuration is altered. Some options are available after the recording for export the camera data in the FLIR Researcher software, like digital levels counting (counts), temperature, and radiance. In this work, the major interest is related to temperature since the surface emissivities are not known in order to infer the temperature measurements directly. In our case, we assume emissivity equals to unity, knowing that literature mentions emissivity value of equivalent gel of 0.92 [5].

Twenty-two frames are obtained from a thermal video, with about 33 ms between each frame and a total duration of 696 ms. The frame with mean temperature peak is considered the initial instant for the model, or $\overline{\theta}(\tau = 0) = \overline{\theta}_0$. The energy applied by the flashlight is not part of the model directly, only the initial mean temperature is, so our problem is to estimate a cooling coefficient for the lumped model. The frame is detected with the greater mean temperature value and all frames before it is discarded for the simulations. To study the temperature distribution in all regions delimited by each unity of mold, the mean temperature is calculated for each frame in each one of the detected molds. The experimental data $\Delta\overline{\theta}_i = \overline{\theta}_i / \overline{\theta}_{max}$ is the representation of the mean values for each contour detected from the peak of temperature (after the flashlight pulse effects). Each one of the values of the measurement vector $\mathbf{Y}_{meas}$ is a result of a normalization according to equation (9):

$$\Delta\,\bar{\theta} = (\bar{\theta}_i - \bar{\theta}_{min})/(\bar{\theta}_{max} - \bar{\theta}_{min}) \tag{9}$$

where $i = 0, \ldots, n$, n is the frame number after flashlight. The index *max* represents the maximum value to all means temperatures calculated for each frame, and the index *min* is the nonzero minimal temperature for all frames. With an algorithm developed to detect contours with the Python library *scikit-image*, it is possible to detect three different mold contours. $\boldsymbol{Y}_{meas}$ is calculated for each one of them to be used later in the parameter estimation routine. At first, a thresholding is applied in a copy of the thermal images turning to zero all temperatures smaller than the minimal temperatures (Figure 5(a)). Then the function *measure.find_contours* from *scikit-image* is used to detect the contours (Figure 5(b)). Finally, the function *polygon2mask* from the same library is used to convert all contours in areas (Figure 5(c)). These regions are matrix with pixel values equal to one in the region and zero outside of them, and they are

combined with the temperature measurement to define the region for calculation of the mean values for the temperatures in each one of the molds.

Markov Chain Monte Carlo (MCMC) Method is used to obtain the parameter estimation under the Bayesian framework, and the Metropolis-Hasting sampling algorithm is used to sample the posterior distribution. Three parameters are considered to determine, namely volumetric heat capacity ρc_p, heat transfer coefficient h, and radius of the mold r (8). All these three parameters are considered random variables with Gaussian prior distribution. The prior for the heat transfer coefficient is considered the same for each mold detected and has been evaluated at 16.5 ± 3.3 $W \cdot K^{-1} \cdot m^{-2}$ with the help of theoretical correlation [6]. A methodology based on [7] is used with the prior of ρc_p. The values for the mean of each radius are inferred based on the size of the contour, just like the standard deviation, for the three-contour detected. Table 1 shows the Gaussian priors for each detected mold.

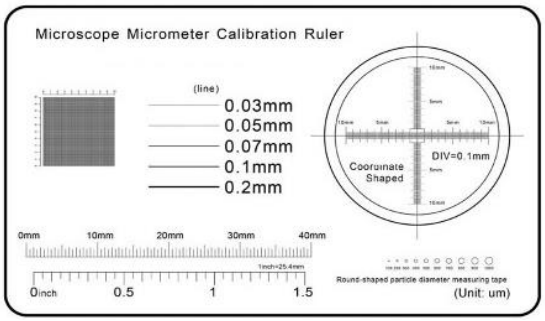

Figure 4: *Ruler used to calibrate the pixel size.*

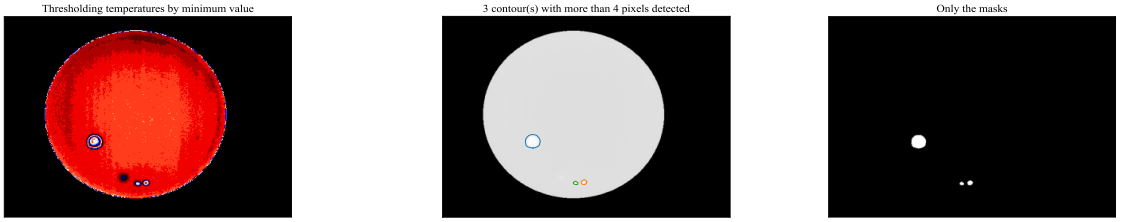

(a) Thresholding *(b) Contours detection* *(c) Only regions detected*

Figure 5: *Contour detection.*

Mold Number	r, mm	ρc_p, $J \cdot K^{-1} \cdot m^{-3}$
	Mean ± Standard Deviation	Mean ± Standard Deviation
1	4.32 ± 0.27	1 500 ± 450
2	1.54 ± 0.09	4 000 ± 1 200
3	1.15 ± 0.07	5 000 ± 1 500

Table 1: *Gaussian priors for the parameters.*

Also, the standard deviation for the Gaussian likelihood function is calculated depending on the standard deviation for the first frame, before the flashlight and with value of σ_{like} = 1.22 %. It is used 3 000 000 samples with a burn-in of 2 100 000 samples. Hence, 900 000 final states are used to calculate the statistics for the parameters. The MCMC method is used separately for each one of the three detected molds and were adjusted to result in acceptance rates around 30% of the candidate points [7]. The acceptance of the samples is 32 %, 20 %, and 13 %, respectively, for mold 1, 2, and 3. Because we have used a low-cost computational model for the direct problem, all simulation is done in about 2 minutes for each one of the detected contours, totalizing about 6 minutes to run the MCMC method in a 11th generation Intel® Core™ i5 @2.40 GHz 4 core and 16 GB RAM computer.

4. Results and discussion

The Markov Chains can be seen in Figure 6 for each one of the molds grouped for separated parameters. For the radius Figure 6(a), we have the better values for prior information and the convergence for the chains is visible and associated with the respective uncertainties showed in Table 1. The respective distribution is showed in Figure 6(b), where we can see the normal distribution for each one of the radii.

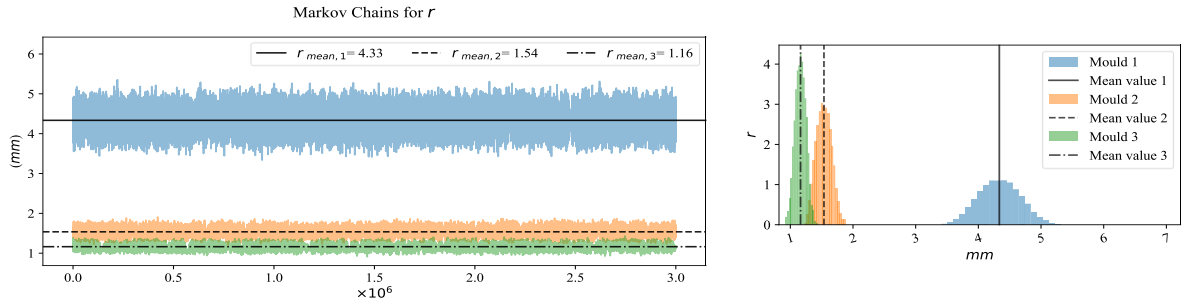

(a) Markov Chains. *(b) Histograms.*

Figure 6: *Radii estimation.*

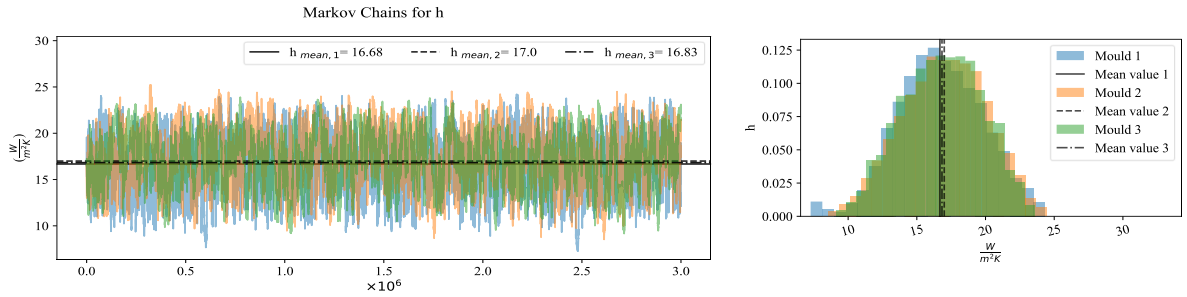

(a) Markov chains. *(b) Histograms.*

Figure 7: *Heat transfer coefficient estimation.*

The heat transfer coefficient has large variation for the three molds, as we can observe in Figure 7(a). Despite this large variation, we can see most of the values well distributed around the mean value for all molds, it is showed clearly in Figure 7(b). The values for h show convergence for chains with large variation. But it is important to consider the difficulty for obtaining this parameter remembering that $h = h_L + h_r$, *i.e.*, i) the convective coefficient depends on the room temperature; ii) there could possibly be air flow around the experimental apparatus, modifying the heat transfer coefficient.

Figure 8(a) shows the results for the volumetric heat capacity. The Markov chains indicate large variation for some of the parameters, mainly for the smallest mold detected. A possible explanation for this behavior is related with the values of the prior standard deviation which is 30 % of the mean value for each mold, and with the smaller mold which shows the larger value of mean and standard deviation, as indicated by Table 1. Also, this information is combined with the information of the mold radius in the exponential model, so when large variation occurs in a specific mold for radius, relatively small variation occurs for volumetric heat capacity. Similarly, to h, the parameter ρc_p presents difficulties in his estimation, yet the posterior probability function is well distributed around the mean values, as we can see in Figure 8(b).

After all simulations, it was possible to estimate the three parameters and the credible interval of 95 %. The summary of these results is show in Table 2. We can observe relatively large values for this credible interval in some results, like ρc_p and h for all molds. Despite the

larger values in Table 2, the mode values can be considered the most credible values for the parameters, and they can be combined to obtain *m*.

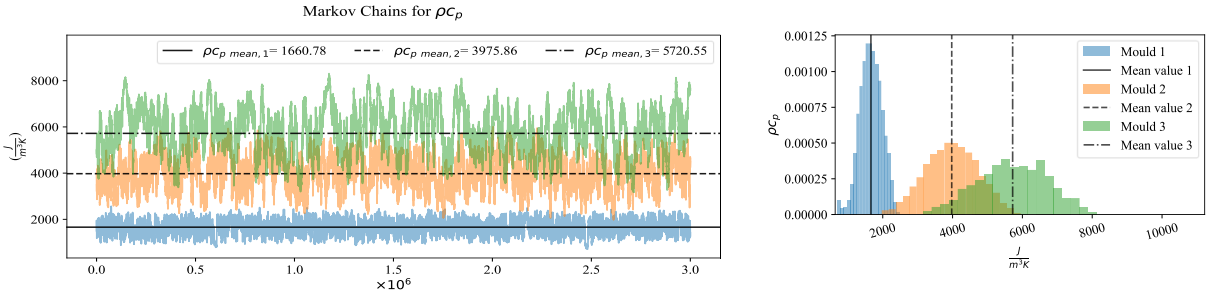

(a) Markov chain *(b) Histograms*

Figure 8: *Volumetric heat capacity estimation.*

Parameters	h_1	h_2	h_3	r_1	r_2	r_3	$(\rho c_p)_1$	$(\rho c_p)_2$	$(\rho c_p)_3$
Mode value	16.67	16.99	16.83	4.33	1.53	1.16	1660.77	3975.85	5720.55
Cred. Interval	10.68	11.04	11.32	3.71	1.31	0.99	1055.24	2517.40	3741.03
of 95 %	22.76	22.59	22.10	4.96	1.76	1.32	2243.59	5389.55	7562.13
Units	$W \cdot K^{-1} \cdot m^{-2}$			mm			$J \cdot K^{-1} \cdot m^{-3}$		

Table 2: *Gaussian posterior for the parameters.*

Figure 9 shows the temperature distribution of the direct problem after the parameter estimation using the mean value and the associated uncertainties based on these parameters. The figure also shows the mean value obtained by the measurements done by the thermal camera. The plots are accompanied by images of the position and size of the fungus on the right, and these images indicate the *m* exponent for the parameter and the respective mold area. It is visible in Figure 9 the better fit is for the larger mold 1, despite two points are outside the gray region of the uncertainties. For molds 2 and 3, even when the mean value does fit quite well, all measured values are inside the uncertainty's regions. This bad fitting could be regarded to thermal interactions between the mold volume and temperature fluctuations in the environment given their small sizes. Additionally, when the area is small, the mean value for them cannot be so representative as in the cases for large ones, for example, mold 1.

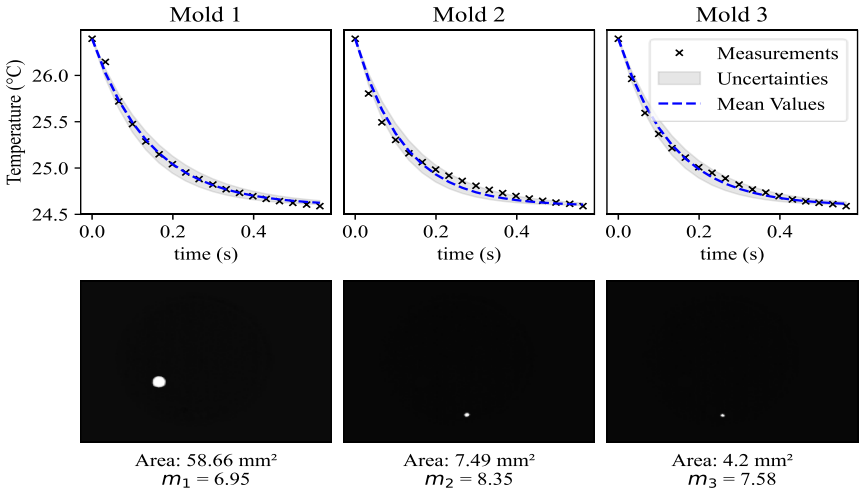

Figure 9: *Temperature distribution and measurements.*

Conclusion

In this work, it was possible to mount an experimental apparatus able to detect molds in a petri plate using a flashlight and a thermographic camera. As well it was developed an algorithm

to detect relatively large thermal responsible molds surfaces estimating their sizes and their respective associated uncertainties. Also, a lumped model analysis was used to predict the cooling of these molds and the parameters for each one of the detected molds were obtained by the Metropolis-Hastings and MCMC method. The estimated parameters were in accordance with the mean values of the camera measurements and better results for this fitting were more visible for larger molds. This preliminary work is important to take the next step in the direction of bacterial colonies detection, thermophysical parameter estimation for these colonies and further prediction of colony growth. To follow the general objective in future works implies the study of better configuration for detect smaller elements in the plate and the application of the growth modelling to estimate not only the sizes of the colonies but also the prediction of the counting for the colonies at future times.

References

[1] S. S. Kumar and A. R. Ghosh, "Assessment of bacterial viability: A comprehensive review on recent advances and challenges," *Microbiology (United Kingdom)*, vol. 165, no. 6, pp. 593–610, Jun. 2019, doi: 10.1099/MIC.0.000786/CITE/REFWORKS.

[2] BS EN 14683:2019, "Medical face masks. Requirements and test methods.," *Standard*, vol. 1, no. 14683. BSI, London, Aug. 31, 2019. Accessed: Oct. 06, 2022. [Online]. Available: https://knowledge.bsigroup.com/products/medical-face-masks-requirements-and-test-methods-1/standard

[3] J. Kaipio and E. Somersalo, *Statistical and Computational Inverse Problems*. Springer Science & Business Media, 2006.

[4] D. Gamerman and H. F. Lopes, *Markov chain Monte Carlo: stochastic simulation for Bayesian inference*. CRC Press, 2006.

[5] S. Hou, *Photo-thermally enhanced temperature gradient gel electrophoresis for DNA separation*, thesis, Notheastern University, Boston Massachusetts, 2018.

[6] F. P. Incropera, *Fundamentals of Heat and Mass Transfer*. John Wiley & Sons, 2011.

[7] S. Brooks, A. Gelman, G. L. Jones, and X. Meng, *Handbook of Markov Chain Monte Carlo*. Boca Raton, FL, USA: Chapman & Hall/CRC, 2011.

Acknowledgements

The support provided by CNPq and FAPERJ, agencies of the Brazilian and Rio de-Janeiro state governments, as well as of DGI of Universidad Santiago de Cali, Colombia is gratefully appreciated. Also, the Brazilian company Baktron laboratory, for provide us materials for the experiments.